A Symmetry-Based Unscented Particle Filter for Rapid State Estimation for SAL Guided Vehicles

Jose A. Rebollo
Dpto. de Ingenieria Aeroespacial, Universidad de Sevilla, Spain.

Francisco Gavilan
Dpto. de Ingenieria Aeroespacial, Universidad de Sevilla, Spain.

Rafael Vazquez, Senior Member, IEEE
Dpto. de Ingenieria Aeroespacial, Universidad de Sevilla, Spain.

***Abstract*—The state estimation problem for vehicles with highly uncertain initial conditions and limited, varying sensors is crucial for both aircraft and spacecraft navigation. This work introduces a Locally Linearized Particle Filter based on a quaternion-adapted Unscented Kalman Filter to estimate the state of a free-fall laser-guided bomb with minimal sensors and uncertain initial conditions. The available sensors include accelerometers, gyroscopes, a barometric altimeter, and a semi-active laser (SAL) receiver that activates only when the target is close and within line-of-sight. Assuming no communication between the carrier aircraft and the bomb (so that the aircraft cannot feed the bomb its launch position and velocity), the algorithm exploits the problem's symmetry to rapidly reconstruct the relative position, velocity, and attitude of the target, even with uncertain initial conditions and insufficient sensor data. In addition, the filter initiates an identification algorithm to estimate the ballistic coefficient, which predicts the miss distance. The proposed algorithm shows promising results in Monte Carlo simulations, quickly converging to an accurate trajectory estimate and providing a high quality aerodynamic model and future trajectory predictions.**

***Index Terms*—Ballistic vehicles, particle filter, unscented Kalman filter, symmetry-based observer, navigation problem, attitude estimation, system identification.**

I. Introduction

Precision-guided munitions (PGMs) have revolutionized the modern warfare, allowing for precise targeting while minimizing collateral damage. Indeed, guided missiles and bombs can be considered everyday weapon systems, present in the inventory of all modern armies. Nowadays, thanks to the miniaturization of electronics and the rising of unmanned aviation, there is a noticeable interest in the development of small-sized and low-cost guided missiles and bombs, paving the way for a cost-effective implementation of these weapons systems in small and versatile tactical unmanned aircrafts. In this regard, among all the wide variety of existing sensors for target positioning (see [1]), Semi-Active Laser (SAL) seekers (especially the strapdown mountings) have emerged as an efficient technology, well suited for small and low cost weapon systems [2]. SAL guidance utilizes a laser designator, which can be positioned either airborne or ground-based, to illuminate the target with a focused laser beam. The missile's seeker, located in its nose, detects the direction of the reflected laser light, providing information about the Line of Sight (LOS) angles between the target and the seeker.

The design of guidance systems for SAL-based weapons has been widely studied in the literature, and there are classical guidance laws that have been successfully employed in practice (a review can be found in [3]). Furthermore, the performance of guidance systems is enhanced by using gimbaled seekers (which directly enable for the application of well-known Proportional Navigation laws, and its variants) and accurate inertial navigation systems (which can also be aided by GNSS sensors, and by the carrier aircraft navigation system through an umbilical link), providing precise measurements of attitude angles, position and velocity, that can be used by the guidance law.

However, measuring additional states for low-cost and small-sized bombs or missiles can pose a challenge. For example, the inertial sensors used in such weapons, which often rely on less-accurate MEMS sensors, do not provide sufficient precision to reconstruct the weapon's status throughout the entire flight, from takeoff, owing to the significant bias that would accumulate. One possible solution would be to use an umbilical link to acquire the first fix from the launch vehicle. Nevertheless, it may not be cost-effective due to the need for a complex aircraft-weapon integration process. But even if the initial launch fix were accessible, the weapon's inertial system could face challenges due to the considerable initial accelerations from the rocket engine or bomb ejection rack. This can result in saturation of low-cost accelerometers or gyros.

Due to the challenges of integrating a full inertial navigation system onto small, SAL-guided weapons, there is growing interest in developing guidance strategies that rely solely on Line-of-Sight (LOS) measurements from the seeker. For instance, the IACCG guidance law introduced in [4] utilizes only LOS angles and rates (which can be estimated using filters, as shown in [5]), while the Bearing-Only IACG approach suggested in [6] requires only LOS angles. Similarly, Reference [7] presents a guidance method for impact angle control based solely on bearing measurements, augmented with a Tobit Kalman Filter to improve estimation of the look angle, LOS an-

Manuscript received XXXXX 00, 0000; revised XXXXX 00, 0000; accepted XXXXX 00, 0000.
(Corresponding author: F. Gavilan). All authors contributed equally.

J. A. Rebollo, F. Gavilan and R. Vazquez are with the Department of Aerospace Engineering, Universidad de Sevilla, 41092 Sevilla (Spain). E-mail: (jrebollo@us.es; fgavilan@us.es; rvazquez1@us.es).

Color versions of one or more of the figures in this article are available online at http://ieeexplore.ieee.org.

gles, and rates. While these methods demonstrate promising performance, the accuracy and robustness of SAL-guided weapons could be further enhanced by incorporating full knowledge of the weapon's state, including its position relative to the target. This would enable optimized flight trajectories, navigation beyond the seeker's visual field, and real-time prediction of miss distance.

In this context, this work aims to contribute to the development of low-cost laser-guided weapons. Specifically, it will focus on the development of a state estimation system for a free-fall bomb (but the presented technique could also be extended to missiles). Such a system is assumed to have on-board inertial sensors (three accelerometers and three gyroscopes), together with a barometric altimeter, but it is assumed that it has neither GNSS, nor an umbilical link with the carrier plane (which would enable data sharing with the airplane navigation system, and hence could provide the bomb with an accurate estimation of its state at the launch time). Consequently, there is great uncertainty about the launch position, attitude and velocity (it is only assumed that the launch is performed within the launch acceptability region, which allows to ensure the capture of the laser beam during the ballistic fall, and whose estimation is out of the scope of this paper, see [8] to illustrate this problem). This prevents the use of conventional filtering techniques to propagate the measurements obtained by the inertial sensors, so that the bomb's state would be rather uncertain during the ballistic fall.

As for the laser seeker, a strapdown configuration is assumed (which is simpler mechanically and reduces costs), so that it provides the LOS angles of the target (with respect to the bomb's body frame). It is also assumed that LOS rates can be obtained from the seeker (which, as will be explained later, is required for fast convergence). Although the problem of line-of-sight (LOS) rate reconstruction is not a trivial one (and is prone to uncertainties), it has been widely studied the literature and there are several techniques which successfully address this issue (see, for instance [9], which proposes a fifth-degree cubature Kalman Filter estimation method based on an augmented-dimensional state model to estimate the LOS rates; [10], which presents a LOS reconstruction filter based on an exact LOS dynamic model of strapdown seeker; or [11], in which this problem is addressed through the development of a line-of-sight rate extended Kalman filter, which was able to accommodate significant time delays due to the processing requirements of computer vision algorithms of the seeker).

Finally, the SAL seeker's effectiveness is assumed to be limited to distances below a certain detection threshold, which is typically less than standard bombing ranges. This means that the bomb initially flies "blind" during the first portion of its ballistic trajectory, lacking target position information. The bomb eventually detects the laser beam at some point along its trajectory, gaining information about the target's relative location. It is at this point that traditional guidance laws (like those previously described) would typically engage, utilizing LOS measurements to adjust the control fins. However, this work demonstrates that, by briefly remaining uncontrolled after laser detection, the bomb can leverage the collected measurements to rapidly reconstruct its complete state. This reconstructed state enables the potential implementation of more sophisticated guidance strategies (which are beyond the scope of this paper).

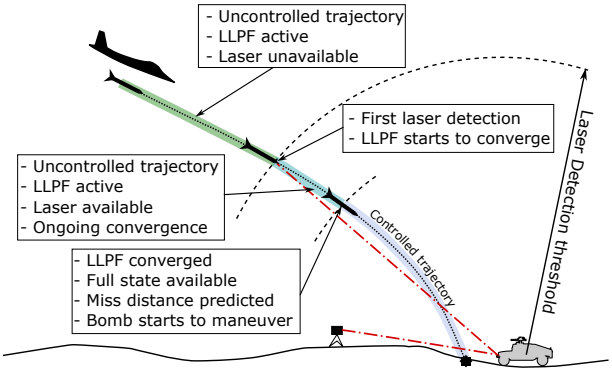

Fig. 1. Problem statement.

This work proposes a full state estimation system implemented as a Locally Linearized Particle Filter (LLPF) based on a quaternion-adapted Unscented Kalman Filter (UKF). This system leverages geometric and aerodynamic symmetries inherent to uncontrolled ballistic flight (described in detail later) to achieve local invertibility. This, in turn, enables very rapid filter convergence once the laser receiver becomes active. As depicted in Fig. 1, upon detecting the laser beam, the proposed guidance system would briefly delay maneuvering to ensure filter convergence. This delay stems from the LLPF formulation, which requires, among other hypotheses, that the bomb maintain zero angle of attack. Once convergence is reached, state propagation can continue using conventional methods, such as an Extended Kalman Filter. This approach provides a reliable state estimate at the cost of slightly reducing the time available for maneuvering. This estimate can then be used by more sophisticated control systems to achieve improved guidance accuracy.

Particle filters, also known as Sequential Monte Carlo methods, have emerged as powerful tools for state estimation in dynamic systems (see [12] for the basis). Among many advantages, they are well-suited for systems with non-linear dynamics and non-Gaussian noise, which can be challenging for traditional filters like the Kalman filter. They also excel in situations where the initial state is highly uncertain, by representing the state estimate as a set of particles dispersed over the state space, they can capture and reduce this initial uncertainty as new measurements are received. These features make this kind of filters especially well posed for a wide variety of tracking and estimation problems (see, for instance, [13], [14]), where nonlinearities arise, and which are oftentimes under high uncertainty levels. Improved versions of Particle Filters for highly nonlinear problems, well suited for engineering

applications, have been proposed. In particular, in [15], an Unscented Particle Filter (UPF) was introduced. This method approximates the computation of the optimal particle weights through implicit local linearization, namely, utilizing the strengths of the unscented transform, together with a Kalman Filter. The aerospace applications of Particle Filters are as diverse as astronomy and remote sensing [16], bearings-only tracking of vehicles [17], ballistic missile tracking [18], navigation in GNSS-denied environments [19], space object tracking [20], attitude determination of space objects using light curves [21], space debris detection in optical astronomical images [22], or attitude estimation of tumbling space objects [23]. However, to the authors' knowledge, there is no previous work considering this particular problem, in which the complete state reconstruction of a SAL guided weapon (having neither GNSS sensors nor an accurate initial fix).

The main contributions of the present work are twofold. First, a LLPF that exploits the symmetries of the problem with a minimal and reasonable number of sensors, under realistic conditions for the activation of the laser receiver, is formulated. Secondly, this LLPF is based on an UKF which is tailored to the specific problem, in particular respecting the invariants arising due to the use of quaternions, even though other such filters already exist (see, for instance, [24]). Simulations show an excellent performance of the algorithm under reasonable sensor noises and initial uncertainties, with the estimation rapidly converging to an accurate estimate of the real trajectory when the laser receiver becomes active. Finally, a system identification algorithm for the drag coefficient and a trajectory predictor are also proposed, that would be of high interest for guidance. This work is an updated and extended version of the conference paper [25].

The structure of this paper is as follows. Section II establishes the basic notation and definitions used throughout the paper, provides system and sensor models for the problems under consideration, and gives a detailed statement of the estimation objective. Next, in Section III, a procedure to determine the state by exploiting constraints and symmetries is developed. Section IV introduces the Particle Filter, providing details of the particular algorithm implemented to solve the problem, including the quaternion-adapted UKF tailored to the specific system models. In section V, a system identification strategy for the vehicle's aerodynamics is proposed as to implement a state prediction algorithm. Simulation results are given in Section VI, and the paper is closed in Section VII with some concluding remarks.

II. Problem statement

This Section serves to both introduce the equations needed for the trajectory and measurements characterization and present the notation which is used throughout this paper.

Regarding notation, vectors are denoted by bold variables. A vector $\boldsymbol{a}$ evaluated in a reference frame (A) is written as $\boldsymbol{a}^A$, while its components are given by $a_j^A, j = 1, 2, 3$.

In this study, we address the state estimation problem for an aircraft-dropped free-fall ballistic vehicle (BV), which could be the case of a laser-guided bomb. The BV's trajectory could also contain some guided segments, but this guidance is not taken into consideration in this work. The vehicle is modeled as fixed mass rigid body subject to free fall motion in a real atmosphere. As shown in Figure 2, O^B is defined as the center of mass of the BV, while O^S is the illuminated target. Three reference frames are considered for convenience. Firstly, the *Surface* (S) reference frame is centered in O^S and moves along with the Earth's surface. The z_S axis points towards the center of the Earth while x_S and y_S are oriented arbitrarily following a right-hand structure. Secondly, the *Body* (B) frame is centered in O^B, and rotates with the BV. Considering a cylindrical shaped BV with a vertical plane of symmetry, x_B is aligned with the longitudinal axis, frontwards; z_B lies in the plane of symmetry, downwards; and y_B points rightwards, fulfilling a right-handed frame. Finally, a generic *Inertial* (I) reference frame is considered, with arbitrary center and orientation. The effect of the Earth's rotation is minimal, so that the relative angular velocity between frames S and I can be approximated to zero. For this particular problem, the expected flight time of the BV is of less than one minute, thus the effective rotation of the Earth with respect to an inertial frame during that time interval is clearly imperceptible.

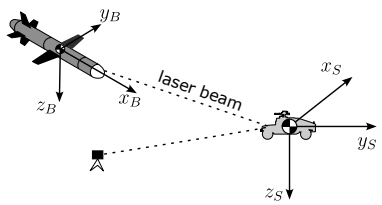

Fig. 2. Reference frames.

Let $\boldsymbol{X}^S$ be the position of the center of mass of the BV referred to (S). Let $\boldsymbol{V}^S = \dot{\boldsymbol{X}}^S$, and $\boldsymbol{V}^B$ its components in B. Let $\boldsymbol{\omega}^B$ be the angular velocity of the BV relative to an inertial frame or, equivalently, to S. $\boldsymbol{A}_G^B$ and $\boldsymbol{A}_{NG}^B$ are defined as the gravitational and non-gravitational inertial accelerations in O^B. For the attitude representation, the attitude quaternion q of the B frame with respect to S is used (see, for instance, [26]).

For the current problem, some additional simplifying hypotheses can be made, without introducing appreciable errors. On the other hand, if the Earth's curvature is neglected, by approximating the Earth's surface by its locally tangent plane, the gravitational acceleration is always aligned with $\boldsymbol{k}_S$, this is, the third vector of the S canonical basis. Finally, no wind is considered in this implementation. While a system identification algorithm similar to the one described in Section V could be used to compute a wind model in real time, this is left out of this work to avoid even more additional complexities and

better focus in the challenges posed by the state estimation problem. From the considered hypotheses, the equations of motion of the BV are reduced to

$$\dot{\boldsymbol{X}}^S = \boldsymbol{V}^S, \tag{1}$$

$$\dot{\boldsymbol{V}}^B = -\left(\boldsymbol{\omega}^B\right)^\times \boldsymbol{V}^B + A_G \boldsymbol{k}_S^B + \boldsymbol{A}_{NG}^B, \tag{2}$$

$$\dot{q} = \frac{1}{2} q \otimes \begin{pmatrix} 0 \\ \boldsymbol{\omega}^B \end{pmatrix}. \tag{3}$$

Note that $\boldsymbol{k}_S^B$ is the $\boldsymbol{k}_S$ vector evaluated in the B reference frame. A_G is the standard mean gravitational acceleration in the Earth's surface. The $\otimes$ operator denotes the quaternion product. Rotations between reference frames can be performed by using the quaternion rotation operator (see [26]).

In order to compute the state of the BV, several onboard sensors are available: a set of 3 accelerometers and 3 gyroscopes, a barometric altimeter and a laser receiver (providing just bearing angles to the target). For ideal sensors, not including measurement errors, which are characterized later, the corresponding ideal measurement models can be written as

$$\boldsymbol{A}_{Acc}^B = \dot{\boldsymbol{V}}^B + \left(\boldsymbol{\omega}^B\right)^\times \boldsymbol{V}^B - \boldsymbol{A}_G^B, \tag{4}$$

$$\boldsymbol{\omega}_{Gyr}^B = \boldsymbol{\omega}^B, \tag{5}$$

$$h_{Baro} = -X_3^S, \tag{6}$$

$$\gamma_1 = \arctan 2(X_3^B, X_1^B), \tag{7}$$

$$\gamma_2 = \arctan 2(X_2^B, X_1^B), \tag{8}$$

where $\arctan 2(y, x)$ is a variation of the arctangent function which avoids singularities (see [27]). Vector $\boldsymbol{A}_G^B$ is the gravitational acceleration expressed in the B basis. If the trajectory starting point was known, without considering error accumulation and with an exact model for gravity, the accelerometer and gyroscope measurements suffice to solve the Navigation Problem. For that reason, these two vectors define the propagation measurements, Z_p, so that

$$Z_p = \begin{pmatrix} \boldsymbol{A}_{Acc}^B \\ \boldsymbol{\omega}_{Gyr}^B \end{pmatrix}. \tag{9}$$

As for the laser measurements, the laser beam deviation from the vehicle's main axis is measured in terms of two angles, which are referred to as γ_1 and γ_2, corresponding to the deviation of the laser direction from the x_B axis projected in the $x_B z_B$ and $x_B y_B$ planes, respectively. The LOS angles measurements are not always available during the BV's operation. In particular, two conditions must be satisfied. Firstly, the laser path must be reasonably aligned with the BV longitudinal axis, so that the LOS measurements are inside the so called Field of View (FOV) of the optical sensor used ([28]). In this application, the FOV is of 15 degrees for each angle. Secondly, the distance from the point source to the sensor must not be larger than a detection threshold which, in this case, is considered of $2500\,\mathrm{m}$. Thus, only if $-15^\circ < \gamma_1, \gamma_2 < 15^\circ$ and $\|\boldsymbol{X}^S\| < 2500\,\mathrm{m}$, the LOS angles can be considered.

For reasons that are detailed later, the time derivatives of h and γ_i are of interest, despite that they are not directly measured. Considering the kinematic evolution, these values are given by

$$v_h = \dot{h} = -V_3^S, \tag{10}$$

$$\dot{\gamma}_1 = \frac{X_1^B \frac{d}{dt} X_3^B - X_3^B \frac{d}{dt} X_1^B}{\left(X_1^B\right)^2 + \left(X_3^B\right)^2}, \tag{11}$$

$$\dot{\gamma}_2 = \frac{X_1^B \frac{d}{dt} X_2^B - X_2^B \frac{d}{dt} X_1^B}{\left(X_1^B\right)^2 + \left(X_2^B\right)^2}. \tag{12}$$

Note that, the time derivative of position in body axes requires the addition of an inertial term, so they must be computed using the following expression:

$$\frac{d}{dt}\boldsymbol{X}^B = -\left(\boldsymbol{\omega}^B\right)^\times \boldsymbol{X}^B + \boldsymbol{V}^B. \tag{13}$$

As the angular velocity is continuously measured and the position, velocity and attitude are state variables, $\dot{\gamma}_1$ and $\dot{\gamma}_2$ are completely defined provided the state is known. Note that, as (h, γ_1, γ_2) only depend on geometric parameters, while $\left(\dot{h}, \dot{\gamma}_1, \dot{\gamma}_2\right)$ also depend on both linear and angular velocities, this second set of parameters can not be obtained by algebraic combination of the first one and vice versa, consequently guaranteeing that these 6 measurements are independent, or what is the same, they provide information that is not cross correlated. This result is proved to be of great interest later on.

III. State determination from constraints and symmetries

This section describes the proposed measurement extension, based on symmetries and constraints, which is a major contribution of this work and allows a fast convergence of the estimator.

Let X be the 10-uple of magnitudes defining the BV's state to be estimated, defined as

$$X = \begin{pmatrix} \boldsymbol{X}^S \\ \boldsymbol{V}^B \\ q \end{pmatrix}. \tag{14}$$

Note that, since X does not belong to a vector space (as it contains the components of an attitude quaternion, which belongs to the space of a 4-D hypersphere, see [26]), the state of the BV has 9 degrees of freedom.

If no initial fix were available, a set of 9 independent equations derived from measurable magnitudes would be needed to fully characterize X. As described in Section IV, the proposed navigation system must be initialized to some state distribution, though with high uncertainty. Generally, a recursive estimation algorithm does not need local invertibility as a condition for convergence. However, local invertibility is of high interest, as it enhances the particles' weighting process and leads to a rapid convergence after LOS measurements are available, as will be shown in Section VI. This is highly desirable for applications such as the one considered in this work, and therefore, the goal of this section is to find 9 algebraic

equations for the state variables (by exploiting as much as possible the available measurements and symmetries), enabling the local invertibility.

Despite the BV being equipped with accelerometers, gyroscopes, a barometric altimeter, and a laser seeker, only the last two sensors provide direct measurements of the vehicle's state, yielding three measurement equations at a given time, as described in (6)–(8),

$$Z_a = \begin{pmatrix} h_{Baro} \\ \gamma_1 \\ \gamma_2 \end{pmatrix} = h_1(X). \tag{15}$$

These equations are insufficient to compute X inverting h. For this purpose, a good estimation of the LOS rates, together with the vertical speed, can be computed as described, for instance, in [9], [10], [11] or [29], among others, leading to

$$\dot{Z}_a = \begin{pmatrix} \dot{h}_{Baro} \\ \dot{\gamma}_1 \\ \dot{\gamma}_2 \end{pmatrix} = h_2(X, Z_p), \tag{16}$$

where h_2 is as shown in equations (10)–(12). Note that, besides computational or measurement errors, a higher order derivative of Z_a would not be useful as there appear terms from $\dot{Z}_p$ which are not available and can not be determined.

With 3 additional measurements or constraints, so that $h(X, Z_p)$ is locally invertible for X, the BV's state would be completely determined from the available information on-board.

One interesting property of this estimation problem, which can be applied to reduce the number of unknown variables, is that there is a spatial symmetry. Indeed, on one hand, Z_p depends only on measurements on the B frame. On the other hand, the only vector components written in the S axes in (15)–(16) are X_3^S and V_3^S. Thus, it is useful to consider a rotation of the S reference frame around the z_S axis, so that the B components are unchanged. This situation is represented in Figure 3.

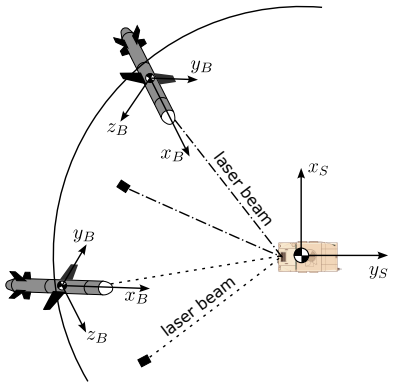

Fig. 3. Rotation of the S reference frame around the z_S axis.

After this transformation (15)–(16) stays invariant and in consequence has a cylindrical symmetry. This means that, with the on-board measurements only, X_1^S and X_2^S can not be computed, as any pair (X_1^S, X_2^S) that satisfies

$$(X_1^S)^2 + (X_2^S)^2 + (h_{Baro})^2 = \|\boldsymbol{X}^B\|^2 \tag{17}$$

can be a solution to (15)–(16) for X. This could be expected, as there is no way to distinguish the x_S and y_S axes. The z_S direction, however, is explicit in (15)–(16) as a consequence of the altimeter's measurements.[1]

Note that, for the current problem, it is of no interest to compute X_1^S and X_2^S independently but the horizontal distance from the BV to the target, $X_h = \sqrt{(X_1^S)^2 + (X_2^S)^2}$, and its relative orientation. Thus, without losing any useful information for guidance, the cylindrical symmetry can be broken by rotating S so that, at any given time,

$$X_1^S = X_h, \tag{18}$$

$$X_2^S = 0. \tag{19}$$

This consideration reduces in 1 the number of degrees of freedom of the system's state without reducing the information available for the guidance system.

In order to determine X, as there are no additional measurements or symmetries, 2 constraints are needed. One useful approach is to benefit from the BV's aerodynamic geometry. Without any control action, the aerodynamic moments tend to align the longitudinal axis of the vehicle with the velocity vector. After a transitory regime, as the wind airspeed is zero, the velocity vector in the B axes can be simplified to

$$\boldsymbol{V}^B = \begin{pmatrix} U \\ 0 \\ 0 \end{pmatrix}. \tag{20}$$

This condition reduces in two the number of unknown variables. Let the additional measurement vector be expanded as

$$Z_a = \begin{pmatrix} h_{Baro} \\ \gamma_1 \\ \gamma_2 \\ \dot{h}_{Baro} \\ \dot{\gamma}_1 \\ \dot{\gamma}_2 \\ 0 \\ 0 \\ 0 \end{pmatrix} = \begin{pmatrix} -X_3^S \\ \arctan 2(X_3^B, X_1^B) \\ \arctan 2(X_2^B, X_1^B) \\ -V_3^S \\ \frac{X_1^B V_3'^B - X_3^B V_1'^B}{(X_1^B)^2 + (X_3^B)^2} \\ \frac{X_1^B V_2'^B - X_2^B V_1'^B}{(X_1^B)^2 + (X_2^B)^2} \\ X_2^S \\ V_2^B \\ V_3^B \end{pmatrix} = h(X, Z_p). \tag{21}$$

It can be proved that the function h is locally invertible for X inside a significant domain (see, e.g. [30]). Therefore, it can be considered that its inverse exists in this region, so that the available measurements allow to compute the vehicle's state if the starting point used to solve the nonlinear problem is close enough to the real state.

These results are sufficient for the proposed PF to rapidly achieve convergence, provided that the number and distribution of particles is adequate to guarantee that at least one particle is inside the region in which the above conditions are satisfied.

[1] In practice, a set of magnetometers or magnetic compass is enough to break this symmetry so that there is a measurable horizontal reference. This is not the case for the considered problem.

IV. Particle Filter formulation

The estimation problem structure is as follows. If the state is known at a given time, its future value can be obtained from the propagation equation,

$$\dot{X} = f(X, Z_p), \tag{22}$$

where $f(X, Z_p)$ is given in equations (1)–(3). The real propagation measurements $\hat{Z}_p$ are corrupted with noise, so that

$$\hat{Z}_p = \begin{pmatrix} \hat{\boldsymbol{A}}^B_{Acc} \\ \hat{\boldsymbol{\omega}}^B_{Gyr} \end{pmatrix} = \begin{pmatrix} \boldsymbol{A}^B_{Acc} \\ \boldsymbol{\omega}^B_{Gyr} \end{pmatrix} + \begin{pmatrix} \delta\boldsymbol{A}^B_{Acc} \\ \delta\boldsymbol{\omega}^B_{Gyr} \end{pmatrix}. \tag{23}$$

The corresponding errors are modeled as samples from white noise Gaussian independent processes (see, e.g. [31]), as given by

$$\delta Z_p = \begin{pmatrix} \delta\boldsymbol{A}^B_{Acc} \\ \delta\boldsymbol{\omega}^B_{Gyr} \end{pmatrix} \sim \mathcal{N}_6(0, \Sigma_p). \tag{24}$$

There are additional measurements, Z_a, which contain information about the trajectory as shown in equation (21), but corrupted by an additive noise sampled from a white Gaussian multivariate distribution,

$$\hat{Z}_a = h(X, Z_p) + \delta Z_a, \tag{25}$$

$$\delta Z_a \sim \mathcal{N}_9(0, \Sigma_a), \tag{26}$$

The Filtering Problem can be stated as follows. From the available measurements, uncertain initial conditions and their expected statistical characteristics, a filtering algorithm must periodically compute the system's state, so that the accessible information is used efficiently. Indeed, for this estimation problem, the initial state probability distribution is widespread, as the initial point is uncertain. Furthermore, the propagation and measurement functions f, g are manifestly nonlinear within this domain, and therefore a linearized Kalman Filter might not be adequate to solve the navigation problem.

The Particle Filter (PF) makes use of the Monte Carlo integration theory and Bayes' Theorem in order to obtain an optimized estimation for nonlinear systems without neither a linear approximation or the Gaussian distribution hypothesis (see e.g. [32]). Instead, it approximates a probability distribution by a set of particles that are propagated and filtered in parallel. The complete probability distribution is obtained by means of a Bayesian approach. This family of algorithms is extensively implemented in applications where it is needed to deal with large uncertainties and nonlinearities, such as tracking from radar data. A Locally Linearized Particle Filter (LLPF) is used as the navigation algorithm for the BV (see [13]). The structure of the proposed filter is similar to an Unscented Particle Filter (UKF), as proposed in [15], but differs substantially in the extension of the methodology for attitude quaternions, which are constrained to norm one, both within the unscented transform and for the weights' computation. Additionally, the structure of the problem is exploited in terms of a symmetry around the vertical axis and additional constraints, leading to a rapid convergence with a low number of samples.

Let $\hat{X}^i_k$ be one estimation of the state, together with a covariance matrix P^i_k, referred to as the particle i, at the time t_k. The algorithm propagates a set of N_p particles that characterize the state probability distribution by using a certain state propagation filter (in this work, as explained below, an UKF scheme is adopted, but other propagation algorithms like an EKF could be explored, see for instance, [33]). The PF assigns to each particle i a positive weight w^i_k, computed by means of a Bayesian approach, that is used to measure the value of a single state estimation within the set of particles. These weights are normalized and used as the probability of each particle in a resampling process, to improve the quality of the set of particles for the next iteration. This whole process is summarized as follows,

- Initial conditions for t_k:

  N_p particles and weights, $\{\hat{X}^i_k, P^i_k, w^i_k\}$

1 Locally linearized KF for each particle:

$$\text{UKF} \rightarrow \{\hat{X}^{i+}_{k+1}, P^{i+}_{k+1}, P^{i-}_{k+1}, P^i_{\nu\nu}\}$$

2 Compute the new particles and weights:

$$\hat{X}^i_{k+1} \sim \mathcal{N}(\hat{X}^{i+}_{k+1}, P^{i+}_{k+1})$$

$$\tilde{w}^i_{k+1} = \frac{f_{\mathcal{N}(h(\hat{X}^i_{k+1}), P^i_{\nu\nu})}(\hat{Z}_k) f_{\mathcal{N}(\hat{X}^{i-}_{k+1}, P^{i-}_{k+1})}(\hat{X}^i_{k+1})}{f_{\mathcal{N}(\hat{X}^{i+}_{k+1}, P^{i+}_{k+1})}(\hat{X}^i_{k+1})}$$

3 Weight normalization and resampling:

$$w^i_{k+1} = \frac{\tilde{w}^i_{k+1}}{\sum_{j=1}^{N_p} \tilde{w}^j_{k+1}}$$

$$\{\hat{X}^i_{k+1}, P^i_{k+1}\} = \text{Resample}(\hat{X}^i_{k+1}, P^i_{k+1}, w^i_{k+1})$$

4 Estimated state:

$$p(\hat{X}_{k+1}|\hat{X}_k, \hat{Z}_k) \approx \sum_{i=1}^{N_p} \frac{1}{N_p} \delta(\hat{X}_{k+1} - \hat{X}^i_{k+1})$$

$$\hat{X}_{k+1} = \sum_{i=1}^{N_p} \frac{1}{N_p} \hat{X}^i_{k+1},$$

where $\delta(\cdot)$ is the Dirac delta distribution. In the algorithm, $f_{\mathcal{N}(\hat{X}^{i-}_{k+1}, P^{i-}_{k+1})}$ refers to the a priori state Gaussian multivariate probability distribution estimated locally for each particle i inside the propagation filter (UKF, in this work), $f_{\mathcal{N}(\hat{X}^{i+}_{k+1}, P^{i+}_{k+1})}$ is the corresponding a posteriori Gaussian multivariate probability density and $f_{\mathcal{N}(h(\hat{X}^i_{k+1}), P^i_{\nu\nu})}$ is the Gaussian multivariate density function for the measurements. Thus, the weights are obtained from the a priori and a posteriori probability distributions, as described next.

As stated above, the selected locally linearized Kalman filter for this application, due to its robustness for nonlinear functions, is the Unscented Kalman Filter (UKF), which has been reformulated to take into account the quaternion attitude representation ([24]).

- Initial conditions for t_k:

$$\hat{X}(t_k) = \hat{X}^+_k, \quad P(t_k) = P^+_k$$

1 Compute and propagate the Sigma Points:

$$\Upsilon_{k,i} = \hat{X}_k \pm \text{cols}(\sqrt{N_p}\text{Chol}(P'_k))$$
$$\dot{\Upsilon}_i = f(\Upsilon_{k,i}, \hat{Z}_p) \rightarrow \Upsilon_{k+1,i},\ Z_i = h(\Upsilon_{k+1,i})$$

2 UKF application:

$$\hat{X}^-_{k+1} = \frac{1}{2N_p}\sum_{i=1}^{2N_p}\Upsilon_{k+1,i}, \quad \bar{Z} = \frac{1}{2N_p}\sum_{i=1}^{2N_p} Z_i$$
$$P^-_{k+1} = \frac{1}{2N_p}\sum_{i=1}^{2N_p}\sum_{j=1}^{2N_p}(\Upsilon_{k+1,i} - \hat{X}^-_{k+1})(\Upsilon_{k+1,i} - \hat{X}^-_{k+1})'$$
$$P_{xz} = \frac{1}{2N_p}\sum_{i=1}^{2N_p}\sum_{j=1}^{2N_p}(\Upsilon_{k+1,i} - \hat{X}^-_{k+1})(Z_i - \bar{Z})'$$
$$P_{\nu\nu} = R + \frac{1}{2N_p}\sum_{i=1}^{2N_p}\sum_{j=1}^{2N_p}(Z_i - \bar{Z})(Z_i - \bar{Z})'$$
$$K = P_{xz}P_{\nu\nu}^{-1}$$
$$\hat{X}^+_{k+1} = \hat{X}^-_{k+1} + K(\hat{Z}_a - \bar{Z}),\ P^+_{k+1} = P^-_{k+1} - KP_{\nu\nu}K'$$

where $\text{Chol}(P)$ denotes the Cholesky decomposition of P. Therefore, the mean and covariance matrix characterizing each probability distribution involved in computing the weights are sampled from the sigma points.

In order to implement the quaternion attitude representation in the state $\hat{X}_k$, several considerations must be made for both the UKF and the PF algorithms. The main idea that allows to extend the UKF and the PF to include quaternions is to use as an auxiliary representation system the attitude vector, which is minimal and does behave like a vector. The state's covariance matrix is computed considering that the attitude is given by a rotation vector $\boldsymbol{\theta}$ (see, e.g. [26]). After the S matrix is obtained, two separate sets of Sigma Points are stored. On one hand, position and velocity are included in the vector Sigma Point V_Υ. On the other hand, the 3 components associated to attitude from each column of S, $\boldsymbol{\theta}_\chi$, are transformed into a quaternion rotation and used to compute the quaternion Sigma Points,

$$q_\Upsilon = \hat{q} \otimes \begin{pmatrix} \cos\frac{\theta_\chi}{2} \\ \frac{\boldsymbol{\theta}_\chi}{\theta_\chi}\sin\frac{\theta_\chi}{2} \end{pmatrix}. \tag{27}$$

Thus, after the Sigma Points are computed, the pair of sets $\{V_{\Upsilon,i}, q_{\Upsilon,i}\}, i \in \{1,\dots,18\}$ are obtained. These Sigma Points can be used to determine the time evolution and the estimated additional measurements using the nonlinear functions f and h without any additional modification.

Computing the covariance matrices involving q_Υ is not immediate, since the definition computing the difference between vectors does not hold for quaternions. In fact, it is necessary to obtain an alternative algorithm to compute the mean of a set of quaternions. Let $\{q_i\}, i \in [1,n]$ be a set of attitude quaternions. Let $\langle q\rangle$ be the mean quaternion. The rotation quaternion r_i from the mean to any of the elements of the set verifies the general rotation composition relation from the Hamilton product

$$q_i = r_i \otimes \langle q\rangle. \tag{28}$$

In consequence, the set of rotation vectors between q_i and $\langle q\rangle$ are given by

$$r_i = q_i \otimes \bar{\langle q\rangle}. \tag{29}$$

Each rotation r_i is equivalent to a rotation vector $\boldsymbol{\theta}_{r,i}$, so that

$$\boldsymbol{\theta}_{r,i} = 2\frac{\boldsymbol{r}_i}{\|\boldsymbol{r}_i\|}\arccos r_{i,0}. \tag{30}$$

Thus, the angle between any reference frame represented by q_i and the mean orientation given by $\langle q\rangle$ is $\theta_{r,i}$. If $\langle q\rangle$ is the mean quaternion, the mean rotation vector $\langle\boldsymbol{\theta}_r\rangle$ must be zero. If $\langle q\rangle$ is not the mean quaternion, $\langle\boldsymbol{\theta}_r\rangle$ is nonzero and oriented towards the real mean direction. Using this property, the mean quaternion of a set can be obtained by using an iterative algorithm, as detailed in [24].

Firstly, an initial guess for the mean quaternion is needed. In the navigation algorithm, the mean of the set of quaternion Sigma Points can be initially approximated by the attitude quaternion q from the prior iteration. Let this starting point be $\langle q\rangle_0$. The set of rotation quaternions r_i is computed from (29). The equivalent rotation vectors $\boldsymbol{\theta}_{r,i}$ are obtained from (30) so that the mean rotation vector is computed from the usual vector definition

$$\langle\boldsymbol{\theta}_r\rangle = \frac{1}{n}\sum_{i=1}^{n}\boldsymbol{\theta}_{r,i}. \tag{31}$$

If the norm of $\langle\boldsymbol{\theta}_r\rangle$ is smaller than a predefined tolerance set to consider that the algorithm has converged, $\langle q\rangle_0$ is accepted as the mean quaternion. Otherwise, the next mean quaternion estimation $\langle q\rangle_1$ is computed rotating $\langle q\rangle_0$ as indicated by $\langle\boldsymbol{\theta}_r\rangle$,

$$q_r = \begin{pmatrix} \cos\frac{\langle\theta_r\rangle}{2} \\ \sin\frac{\langle\theta_r\rangle}{2}\frac{\langle\boldsymbol{\theta}_r\rangle}{\langle\theta_r\rangle} \end{pmatrix}, \tag{32}$$
$$\langle q\rangle_1 = q_r \otimes \langle q\rangle_0. \tag{33}$$

This process is repeated until the mean quaternion is obtained. This technique is very interesting for the current application since the final set of rotation vectors $\boldsymbol{\theta}_{r,i}$ is equivalent to the difference $\boldsymbol{x}_i - \langle\boldsymbol{x}\rangle$ when computing the covariance matrix of a set of vectors $\boldsymbol{x}_i$. Hence, inside the UKF, the term $\Upsilon_{k+1,i} - \hat{X}^-_{k+1}$ is substituted by

$$\Upsilon_{k+1,i} - \hat{X}^-_{k+1} \equiv \begin{pmatrix} \boldsymbol{X}^S_{\Upsilon,k+1,i} - \hat{\boldsymbol{X}}^{S,-}_{k+1} \\ \boldsymbol{V}^B_{\Upsilon,k+1,i} - \hat{\boldsymbol{V}}^{B,-}_{k+1} \\ \boldsymbol{\theta}_{r,i} \end{pmatrix} \tag{34}$$

where $\boldsymbol{X}^S_{\Upsilon,k+1,i}$ and $\boldsymbol{V}^B_{\Upsilon,k+1,i}$ are the position and velocity Sigma Points. After the state change is computed in the Kalman Filter, the three components describing the change in attitude, which are a rotation vector, are converted to a rotation quaternion and applied to the uncorrected attitude quaternion to compute the filtered attitude. With these generalizations, the UKF is extended to include quaternions, so that the basic algorithm stays unchanged.

The LLPF was generalized to include quaternions following a similar reasoning. In this case, the normal multivariate probability distributions, which allow computing the particles' weights, have to be extended to use quaternions as an attitude representation system. This situation appears when evaluating for each particle

$$f_{\mathcal{N}(\hat{X}^{i-}_{k+1},P^{i-}_{k+1})}(\hat{X}^{i}_{k+1}) = \frac{\exp\left(-\frac{1}{2}(\hat{X}^{i}_{k+1}-\hat{X}^{i-}_{k+1})'(P^{i-}_{k+1})^{-1}(\hat{X}^{i}_{k+1}-\hat{X}^{i-}_{k+1})\right)}{\sqrt{(2\pi)^9|P^{i-}_{k+1}|}}, \tag{35}$$

$$f_{\mathcal{N}(\hat{X}^{i+}_{k+1},P^{i+}_{k+1})}(\hat{X}^{i}_{k+1}) = \frac{\exp\left(-\frac{1}{2}(\hat{X}^{i}_{k+1}-\hat{X}^{i+}_{k+1})'(P^{i+}_{k+1})^{-1}(\hat{X}^{i}_{k+1}-\hat{X}^{i+}_{k+1})\right)}{\sqrt{(2\pi)^9|P^{i+}_{k+1}|}}, \tag{36}$$

where $(\hat{X}^{i}_{k+1}-\hat{X}^{i-}_{k+1})$ and $(\hat{X}^{i}_{k+1}-\hat{X}^{i+}_{k+1})$ are not defined for the quaternion part. As written in (28)–(29), the rotation quaternion between two attitude quaternions is easily obtained by using the Hamilton product. The corresponding attitude vector is given by (30). The LLPF can be extended by considering the following equivalences

$$\hat{X}^{i}_{k+1}-\hat{X}^{i-}_{k+1} \equiv \begin{pmatrix} \hat{\boldsymbol{X}}^{S,i}_{k+1}-\hat{\boldsymbol{X}}^{S,i-}_{k+1} \\ \hat{\boldsymbol{V}}^{B,i}_{k+1}-\hat{\boldsymbol{V}}^{B,i-}_{k+1} \\ \boldsymbol{\theta}^{-}_{k+1} \end{pmatrix}, \tag{37}$$

$$\hat{X}^{i}_{k+1}-\hat{X}^{i+}_{k+1} \equiv \begin{pmatrix} \hat{\boldsymbol{X}}^{S,i}_{k+1}-\hat{\boldsymbol{X}}^{S,i+}_{k+1} \\ \hat{\boldsymbol{V}}^{B,i}_{k+1}-\hat{\boldsymbol{V}}^{B,i+}_{k+1} \\ \boldsymbol{\theta}^{+}_{k+1} \end{pmatrix}, \tag{38}$$

where

$$r^{-}_{k+1} = \hat{q}^{i}_{k+1} \otimes \bar{\hat{q}}^{i-}_{k+1}, \tag{39}$$

$$\boldsymbol{\theta}^{-}_{k+1} = 2\frac{\boldsymbol{r}^{-}_{k+1}}{\|\boldsymbol{r}_i\|}\arccos r^{-}_{k+1,0}, \tag{40}$$

$$r^{+}_{k+1} = \hat{q}^{i}_{k+1} \otimes \bar{\hat{q}}^{i+}_{k+1}, \tag{41}$$

$$\boldsymbol{\theta}^{+}_{k+1} = 2\frac{\boldsymbol{r}^{+}_{k+1}}{\|\boldsymbol{r}_i\|}\arccos r^{+}_{k+1,0}. \tag{42}$$

As for $f_{\mathcal{N}(h(\hat{X}^{i}_{k+1}),P^{i}_{\nu\nu})}$, a conventional multivariate Gaussian distribution for vector variables can be used. The described variants allow to completely generalize the LLPF and its corresponding UKF algorithms to use of quaternions as the attitude representation system.

A correction is needed for the imposed symmetry condition, as stated in (18)–(19), which can otherwise be problematic. If $X^S_2 \ll X^S_1$, setting X^S_2 to zero does not change significantly the horizontal distance from the BV to the target, neither the BV's orientation with respect to the S reference system. If, on the contrary, X^S_2 is representative against X^S_1, the considered equation can lead to an undesirable reduction of the distance to the target and an unexpected rotation of the B axes relative to the S axes, thus reducing the algorithm's overall performance. To guarantee that this equation behaves as rotation, the following corrections can be applied. Let $\boldsymbol{X}^S_0$ be the position before applying the filter, and $\boldsymbol{X}^S_f$ its value after the filtering process. The horizontal angle between these vectors can be computed from the definition of the dot product

$$\cos\psi = \frac{\begin{pmatrix} X^S_{0,1} \\ X^S_{0,2} \\ 0 \end{pmatrix} \cdot \begin{pmatrix} X^S_{f,1} \\ X^S_{f,2} \\ 0 \end{pmatrix}}{\sqrt{\left(X^S_{0,1}\right)^2+\left(X^S_{0,2}\right)^2}\sqrt{\left(X^S_{f,1}\right)^2+\left(X^S_{f,2}\right)^2}}, \tag{43}$$

where only the horizontal components were considered. Thus, the corrected distance after filtering is given by

$$X'^S_{f,1} = \frac{X^S_{f,1}}{\cos\psi}. \tag{44}$$

As for the needed attitude correction for q, it can be obtained by introducing a rotation given by

$$q' = \begin{pmatrix} \cos\frac{\psi}{2} \\ 0 \\ 0 \\ \sin\frac{\psi}{2} \end{pmatrix}. \tag{45}$$

Under this algorithm, the particles distribution can be propagated freely from the available information without constraints, and corrected when laser measurements are available. This allows to maintain all the initially available information by propagating the unconstrained particles. When LOS measurements are available, the considered equations are included in the filtering algorithm.

V. Application for ballistic coefficient estimation

Assuming an statically-stable, unpowered and axisymmetric (with respect to its longitudinal axis, X_B) ballistic vehicle, equation (2) can be simplified by neglecting lift and cross forces against drag (notice that the vehicle is also assumed to be flying at zero angle of attack, so that $V^B_2, V^B_3 \approx 0$, and the total aerodynamic force will be aligned with the airspeed vector). Hence, the aerodynamic acceleration can be written as follows

$$\boldsymbol{A}^B_{NG} = -\frac{D}{m_b}\frac{\boldsymbol{V}^B}{|\boldsymbol{V}^B|} = -\frac{p_q}{\beta}\frac{\boldsymbol{V}^B}{|\boldsymbol{V}^B|} \tag{46}$$

where m_b is the vehicle's mass, p_q is the dynamic pressure, and β is the ballistic coefficient, defined as

$$\beta = \frac{m_b}{SC_D}, \tag{47}$$

being C_D the drag coefficient, and S the reference surface.

Notice that, under the aforementioned assumptions, the ballistic coefficient is the single vehicle-dependent parameter appearing in the equations of motion (1)–(3). This is to say, if the initial state were known, the impact point could be predicted if a proper ballistic coefficient model were available. Thus, since the ballistic coefficient would be extremely useful for the design of predictive guidance systems for such vehicles (for instance, those based on MPC, like [34]), the structure of the proposed

LLPF is exploited to also provide an online estimation of β.

To do so, define the drag per unit of mass

$$d = \frac{D}{m_b} = \frac{1}{2m_b}\rho\left(V_1^B\right)^2 SC_D, \tag{48}$$

which depends on altitude (through the air density, ρ) and on the BV's state through C_D. Nonetheless, after the LOS measurements are available, density does not change sensibly and thus can be considered a constant. As both V_2^B and V_3^B are considered zero by the the steady-state attitude condition, a general model for the drag coefficient is assumed to be

$$C_D \propto \left(V_1^B\right)^n. \tag{49}$$

Equations (48) and (49) allow to write

$$d = \alpha\left(V_1^B\right)^{n+2},\ \alpha > 0. \tag{50}$$

If α and n were known, the drag coefficient could be computed from V_1^B and the propagation problem would be solved. As α is necessarily positive, taking the logarithm of both sides and substituting $d = A_{Acc}^B$, one has:

$$\log|A_{Acc}^B| = \log\alpha + (n+2)\log|V_1^B|, \tag{51}$$

It is useful to define the measured vectors and matrices for each iteration

$$y_k = \log|\hat{A}_{Acc,k}^B| \tag{52}$$

$$X_k = \begin{pmatrix}1 & \log|\hat{V}_{1,k}^B|\end{pmatrix}. \tag{53}$$

Similarly, let the estimated coefficients be given by

$$\hat{\boldsymbol{\alpha}}_k = \begin{pmatrix}\log\alpha \\ n+2\end{pmatrix}. \tag{54}$$

This estimation problem can be solved iteratively by means of a Recursive Least Squares (RLS) method. In particular, let the cost function be given by

$$J_k = \sum_{i=1}^{k}\left[\lambda^{k-i}\left\|\boldsymbol{y}_k - X_k\hat{\boldsymbol{\alpha}}\right\|_2 + \lambda^k\left\|\hat{\boldsymbol{\alpha}} - \boldsymbol{\alpha}_0\right\|_{P_0^{-1}}\right], \tag{55}$$

where λ is the forgetting factor and P_0 is the covariance matrix of the initial estimation $\boldsymbol{\alpha}_0$. The optimal solution for the LS problem is recursively computed as

$$P_{k+1} = \frac{1}{\lambda}P_k - \frac{1}{\lambda}P_k X_k'\left(\lambda\mathrm{I} + X_k P_k X_k'\right)^{-1} X_k P_k \tag{56}$$

$$\hat{\boldsymbol{\alpha}}_{k+1} = \hat{\boldsymbol{\alpha}}_k + P_{k+1}X_k'\left(y_k - X_k\hat{\boldsymbol{\alpha}}_k\right). \tag{57}$$

This algorithm can be executed in real time after the BV's state is estimated from the LOS measurements. The initialization point $\boldsymbol{\alpha}_0$ can be obtained by applying a Batch Least Squares (BLS) method to a set of past states generated through a trajectory reconstruction algorithm. It is particularly simple to integrate equations (1)–(3) backwards in time from the present state and using the stored measurements for $\boldsymbol{\omega}_{Gyr}^B$ and $\boldsymbol{A}_{Acc}^B$. For a set of n_{LS} measurements, let X_0 and y_0 be the stacked matrices

$$y_0 = \begin{pmatrix}\boldsymbol{y}_k \\ \boldsymbol{y}_{k-1} \\ \vdots \\ \boldsymbol{y}_{k-n_{LS}}\end{pmatrix} \in \mathbb{R}^{n_{LS}}, X_0 = \begin{pmatrix}X_k \\ X_{k-1} \\ \vdots \\ X_{k-n_{LS}}\end{pmatrix} \in \mathbb{R}^{n_{LS}\times 2}. \tag{58}$$

The initial estimation $\boldsymbol{\alpha}_0$ is computed as

$$\boldsymbol{\alpha}_0 = \left(X_0'X_0\right)^{-1}X_0'y_0. \tag{59}$$

This initialization process allows to compute good predictions from the moment the state is correctly estimated. Note that, although no significant changes are expected for $\hat{\boldsymbol{\alpha}}$ during the RLS, the initial point is not critical, as the forgetting factor can be adjusted to only consider the last set of measurements. In particular, a usual value of λ is of around 0.98. For a sampling frequency of $40Hz$, this means that measurements taken 2 seconds in the past are weighted only a 20% against newly obtained measurements. A higher λ makes the system more robust against noise and perturbations. The situation is similar with P_0, which can be arbitrarily set to the 2-dimensional identity matrix.

VI. Results

To analyze the performance of the proposed algorithm, a simulation model based on a small free-fall bomb has been employed. The aerodynamic model of the bomb has been obtained using semi-empirical methods (as detailed in reference [35]). Given that this work exclusively focuses on the free-fall flight phase (without control), the primary aerodynamic parameter governing the trajectory is the ballistic coefficient, which is illustrated in Fig. 4.

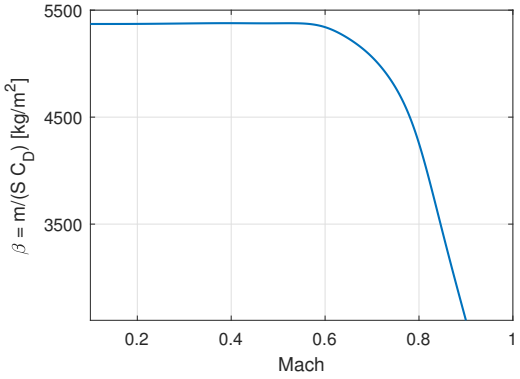

Fig. 4. Ballistic coefficient

Regarding the filter design, a set of $N_p = 200$ particles is considered, with an update frequency of 40 Hz. The complete Particle Filter algorithm is programmed using *C++* to evaluate its computational performance. The available CPU to perform the simulations in this work is an *Intel(R) Core(TM) i7-3537U*. No GPU acceleration was used. With this limited processing capacity, the simulations including the 40 Hz navigation system update rate are executed with a ratio of around 1 second of computation for each 1 simulation second, this is, the algorithm operates in real time. Additionally, a very interesting property of the proposed navigation system is its high degree of parallelizability. Indeed, as described in [36], a Parallel Quaternion Particle Filter (PQPF) could be implemented to effectively reduce the computational time between iterations.

To evaluate the performance of the proposed estimation filter, an in-depth case study and a set of Monte Carlo simulations were carried out. For the single fall analysis, the initial bomb's state is given by

$$\boldsymbol{X}_{0,1}^{S} = \begin{pmatrix} -3670 \\ 0 \\ -2000 \end{pmatrix} \text{ m}, \boldsymbol{V}_{0,1}^{B} = \begin{pmatrix} 200 \\ 0 \\ 0 \end{pmatrix} \text{ m/s}, \quad q_{0,1} = \begin{pmatrix} 1 \\ 0 \\ 0 \\ 0 \end{pmatrix}, \boldsymbol{\omega}_{0,1}^{B} = \begin{pmatrix} 0 \\ 0 \\ 0 \end{pmatrix} \text{ rad/s}. \tag{60}$$

For the Monte Carlo analysis, a grid of initial conditions leading to an eventual LOS sensor availability was generated by back propagating from a grid of final states with varying feasible velocities and pitch angles. In particular, a grid of 32×32 values was considered, leading to 1024 simulations. The considered procedure to generate valid initial conditions gives place to the initial states distribution included in Figure 5. Note that a wide distribution of initial states is considered.

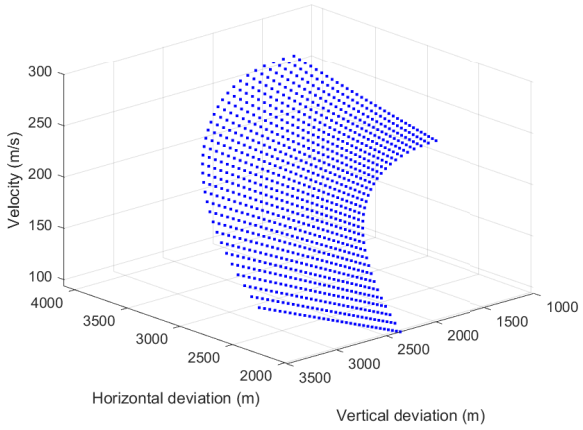

Fig. 5. Distribution of initial conditions in the Monte Carlo simulations

The variances of the additive Gaussian white noise for measurements in all simulations are set to $\sigma_h^2 = 100\,\text{m}^2$, $\sigma_a^2 = 2 \cdot 10^{-2}\,\text{m}^2/\text{s}^4$, $\sigma_\omega^2 = 5 \cdot 10^{-6}\,\text{rad}^2/\text{s}^2$ and $\sigma_\gamma^2 = 5 \cdot 10^{-5}\,\text{rad}^2$. The initial particles distribution is sampled from a Gaussian multivariate state probability density,

$$\hat{X}_0^i \sim \mathcal{N}(\mu_{X,0}, \Sigma_{X,0}), i \in [1, N_p]. \tag{61}$$

The initial bias $\mu_{X,0}$ of the state estimation is of $80\,\text{m}$ for each position coordinate, $15\,\text{m/s}$ for each velocity component and $0.3\,\text{rad}$ for each Euler angle. The covariance matrix is set to

$$\Sigma_{X,0} = \text{Diag}\left(8000\ 8000\ 8000\ 200\ 200\ 200\ 0.05\ 0.05\ 0.05\right)^T.$$

These initial conditions reflect the uncertainty in the starting point of the trajectory.

For the single scenario case study, the computed trajectory of each particle and the final estimated trajectory are included in Figures 6 and 7 for a particular instance of the initial conditions. Note that the LOS measurements are not available during most of the simulation time. The algorithm propagates and filters the particles distribution considering only the information accessible on-board.

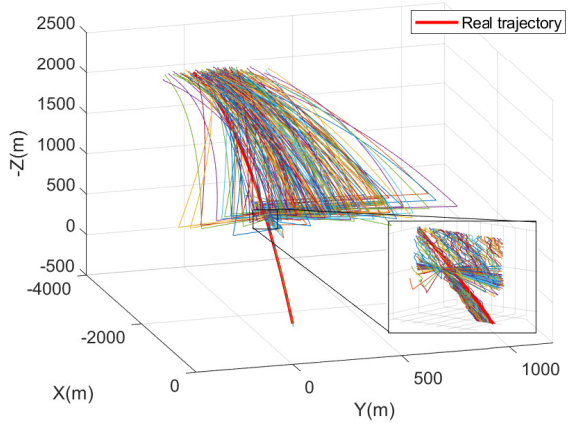

Fig. 6. Path of each particle in the navigation algorithm

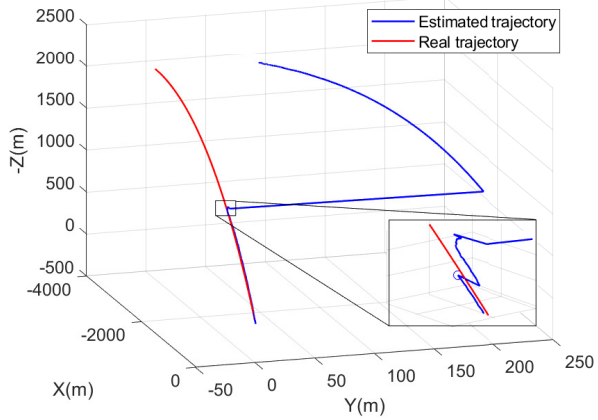

Fig. 7. Path estimation of the complete trajectory in the navigation algorithm. The convergence point of the Particle Filter is circled.

More generally, Figure 8 includes the results of the Monte Carlo simulations. In particular, the distribution of deviations Δr of the impact point estimation at the impact time is displayed. A standard deviation of $3.9662\ \text{m}$ is obtained. Note that this metric is a measure of convergence, rather than being indicative of the precision one might anticipate within a prospective guidance system utilizing this algorithm (commonly measured with the so-called Circular Error Probable or CEP). Moreover, the error is evaluated at the impact point, for which the available set of measurements is the largest. Anyhow, this result shows good convergence behavior of the proposed algorithm for highly uncertain initial conditions.

The proposed navigation algorithm correctly converges to the desired state. Moreover, the time between the initial LOS measurements and the convergence of the estimation to the real state is in most of the simulations very short. In order to characterize this behavior, let $\hat{\boldsymbol{x}}_k^i$ be the estimated position of the i-th particle at iteration

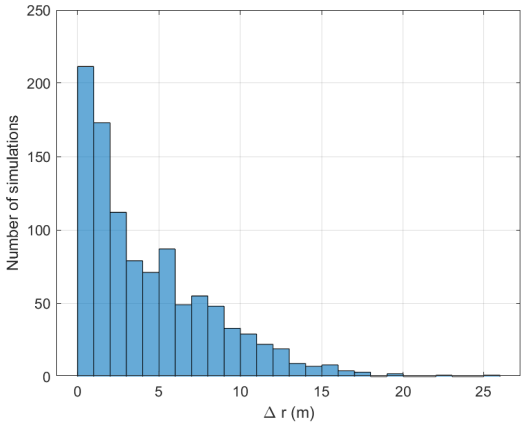

Fig. 8. Position estimation error in the impact point for 1024 Monte Carlo simulations

k. Let Σ_k be the covariance matrix of this distribution. The chosen convergence convergence metric is given by

$$\sigma_k = \sqrt{\mathrm{Tr}\,(\Sigma)}, \tag{62}$$

where Tr is the trace operator, computing the sum of the diagonal terms of a matrix. The proposed metric gives a characteristic magnitude of the size of the particle distribution in the position space. Furthermore, this parameter can be computed on-line and compared to a threshold to evaluate convergence. For this work, a convergence limit of 15 m is considered. Therefore, the convergence time is defined as the difference between the time instant at which σ is smaller than the threshold and the one at which the LOS measurement is first available.

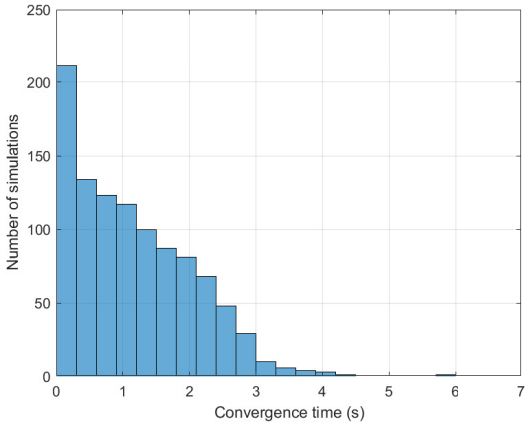

Fig. 9. Convergence times for 1024 Monte Carlo simulations, with standard deviation threshold for particles of 15 m.

As included in Figure 9, the convergence times distribution is concentrated below 3 s, with most simulations presenting a much lower value. In particular, an average convergence time of 1.1526 s is obtained. Consequently, a fast convergence is achieved, enabling the implementation of more advanced guidance algorithms benefiting from the state estimation. This is a consequence of the resampling process. Each time a particle obtains a very good approximation of the BV's state, all the other particles are resampled to that state, as its weight is nearly 1. In this situation, the hypervolume filled by the particles distribution within the state space is significantly reduced. After the resampling step, each particle randomly propagates to a different state, slightly increasing the size of the particles distribution and therefore avoiding degeneracy. This excellent behavior is obtained in a variety of initial conditions, uncertainty and measurement noise. The parameters within the quaternion UKF and the number of particles can be tuned to improve performance for a given computational capacity.

As for the system identification and prediction algorithms, they highly benefit from the rapid convergence of the state estimates. Figure 10 shows the estimation error of the future ballistic coefficient through (46) from the inferred parameters α and n at $t = 17.0$ s, the estimated velocity and altitude. As described in Section V, a forgetting factor of 0.98 is used, together with an initialized P_0 equal to the identity matrix. Furthermore, Figure 11 displays the predicted trajectory at $t = 17.0$ s, together with the actual state evolution. For the impact point, the estimation deviates 18.61 m from the real position. The RLS output coefficients present minor fluctuations, mainly at $t = 16.0$ s, as it could be expected from the arbitrary initialization of P_0. The predicted ballistic coefficient exhibits a good accuracy, with a small deviation from the true value, although a growing bias is observed. Finally, the prediction of the future state fits well the future trajectory. From the estimations provided by the navigation system, the system identification algorithm converges to a model that fits adequately the aerodynamic behavior of the vehicle.

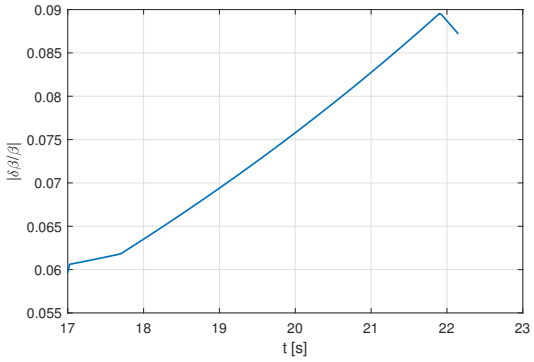

Fig. 10. Relative estimation error of the ballistic coefficient at $t = 17.0$ s.

VII. Conclusions

This work introduced a Locally Linearized Particle Filter, based on a quaternion-adapted Unscented Kalman Filter, to estimate the state of a vehicle with a minimal number of sensors and significantly uncertain ini-

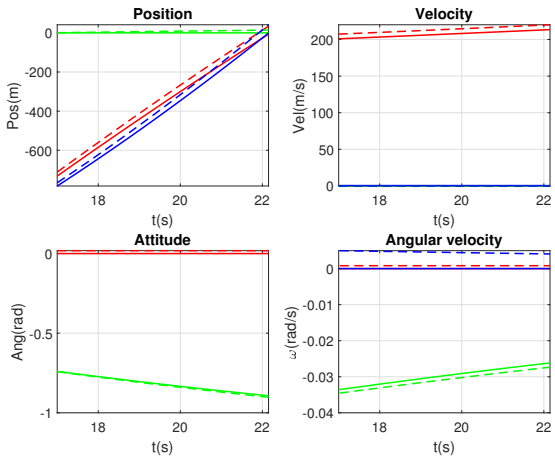

Fig. 11. Future trajectory prediction at $t = 17.0$ s. Vector x, y and z components are plotted in red, green and blue, respectively. Solid lines denote real values, and dashed lines the estimated ones.

tial conditions, exploiting the geometrical symmetries of the problem. The particular case of a ballistic vehicle which is traveling towards a target illuminated by laser was considered. The considered sensors were a triad of accelerometers and gyroscopes, a barometric altimeter, and a laser receiver that only activates when the target is close enough. A symmetry around the vertical axis was identified; based on it, the algorithm was capable of rapidly solving the navigation problem, even with strongly uncertain initial fix and the laser receiver initially not active. The proposed navigation algorithm showed promising results in simulation, rapidly converging to an accurate estimate of the real trajectory when the laser receiver became activated and is capable also of trajectory prediction based on the estimation of the drag coefficient.

The number of particles was set to a few hundred; while this is a small quantity of particles for a PF, the LLPF behaved excellently in Monte Carlo simulations. Thus, if more uncertainties or measuring noise were to be considered, the LLPF could be enhanced by simply increasing the number of particles, and enlarging the initial distribution. This consideration, however, also would increase the required computational cost. Also note that the particles set was sampled from a rather arbitrary probability distribution. In practice, if the envelope of initial states is known a priori, the set of particles can be initialized to coincide with these conditions. In this regard, if the attitude uncertainty is reduced, the algorithm can estimate the system's state with more accuracy. This property is very useful for the proposed application, since the developed estimation algorithm can be easily modified to include any available information about the operation by means of changing the initial probability distribution. Note that the starting set of particles can be adapted to any operational conditions without any specific knowledge on filtering theory nor the algorithms functioning.

This work also implemented a system identification algorithm and a trajectory prediction system, based on navigation system outputs, and verified their performance in simulation. The proposed methods allow obtaining an estimation of the future trajectory as to be considered by a prospective guidance system, adequately fitting the actual aerodynamic behavior of the ballistic vehicle. This framework could be extended to model and identify wind (see also the procedure of [34]), although more stringent requirements on the quality and frequency of the available measurements could be expected, as well as the overall acceptable uncertainty of the navigation system and the precision of the predictions.

These results could be extended to other vehicle state estimation problems, both for aircraft and spacecraft, specially if symmetries can be identified and exploited; two relevant examples include GNSS-denied aircraft navigation or spacecraft rendezvous with non-cooperative tumbling targets such as space debris. In addition, the state estimated by the navigation algorithm would be readily available to be used for guidance and control purposes, which would be a natural next step, both for the proposed application or others.

Acknowledgement

The authors gratefully acknowledge support by grant TED2021-132099B-C33 funded by MICIU/AEI/10.13039/501100011033 and by "European Union NextGenerationEU/PRTR."

REFERENCES

[1] G. Siouris, *Missile Guidance and Control Systems*. Springer New York, 2006.

[2] K. Hubbard, G. Katulka, D. Lyon, D. Petrick, F. Fresconi, and T. Horwath, "Low-cost semi-active laser seekers for us army applications," in *Proceedings of the International Telemetering Conference*, vol. 44, 2008.

[3] H. Pastrick, S. Seltzer, and M. Warren, "Guidance laws for short-range tactical missiles," *Journal of Guidance and Control*, vol. 4, no. 2, pp. 98–108, 1981.

[4] B.-G. Park, H.-H. Kwon, Y.-H. Kim, and T.-H. Kim, "Composite guidance scheme for impact angle control against a nonmaneuvering moving target," *Journal of Guidance, Control, and Dynamics*, vol. 39, no. 5, pp. 1132–1139, 2016.

[5] K. D. S. Raj and I. S. S. Ganesh, "Estimation of line-of-sight rate in a homing missile guidance loop using optimal filters," in *2015 International Conference on Communications and Signal Processing (ICCSP)*, 2015, pp. 0398–0402.

[6] H.-G. Kim, J.-Y. Lee, and H. J. Kim, "Look angle constrained impact angle control guidance law for homing missiles with bearings-only measurements," *IEEE Transactions on Aerospace and Electronic Systems*, vol. 54, no. 6, pp. 3096–3107, 2018.

[7] Y. Lee, S. Lee, Y. Kim, Y. Han, J. Park, and G.-H. Kim, "Capture region of tactical missile equipped with semi-active laser seeker using tobit kalman filter," *IEEE Access*, vol. 10, pp. 11 714–11 729, 2022.

[8] X. Chen, Z. Yang, J. Bao, G. Zhan, W. Huo, and D. Zhou, "Fitting release region of laser guided bomb based on generative adversarial network," in *2022 IEEE International Conference on Unmanned Systems (ICUS)*, 2022, pp. 115–120.

[9] C. Wei, Y. Han, N. Cui, and H. Xu, "Fifth-degree cubature Kalman filter estimation of seeker line-of-sight rate using augmented-dimensional model," *Journal of Guidance, Control, and Dynamics*, vol. 40, no. 9, pp. 2355–2362, 2017.

[10] Z. Lin, Y. Yao, and K.-M. Ma, "The design of LOS reconstruction filter for strap-down imaging seeker," in *2005 ICMLC*, vol. 4, 2005, pp. 2272–2277.

[11] J. M. Maley, "Line of sight rate estimation for guided projectiles with strapdown seekers," in *AIAA GNC Conference*, 2015, p. 0344.

[12] A. Doucet, N. De Freitas, N. J. Gordon *et al.*, *Sequential Monte Carlo methods in practice*, ser. Statistics for Engineering and Information Science. Springer New York, 2001.

[13] B. Ristic, S. Arulampalam, and N. Gordon, *Beyond the Kalman Filter: Particle Filters for Tracking Applications*. Artech House, 2003.

[14] F. Gustafsson, F. Gunnarsson, N. Bergman, U. Forssell, J. Jansson, R. Karlsson, and P.-J. Nordlund, "Particle filters for positioning, navigation, and tracking," *IEEE Transactions on Signal Processing*, vol. 50, no. 2, pp. 425–437, 2002.

[15] R. Van Der Merwe, A. Doucet, N. De Freitas, and E. Wan, "The unscented particle filter," *Advances in neural information processing systems*, vol. 13, 2000.

[16] L. Martino, V. Elvira, J. López-Santiago, and G. Camps-Valls, "Compressed particle methods for expensive models with application in astronomy and remote sensing," *IEEE Transactions on Aerospace and Electronic Systems*, vol. 57, no. 5, pp. 2607–2621, 2021.

[17] T. Brehard and J.-p. L. Cadre, "Hierarchical particle filter for bearings-only tracking," *IEEE Transactions on Aerospace and Electronic Systems*, vol. 43, no. 4, pp. 1567–1585, 2007.

[18] M. Yu, W.-H. Chen, and J. Chambers, "State dependent multiple model-based particle filtering for ballistic missile tracking in a low-observable environment," *Aerospace Science and Technology*, vol. 67, pp. 144–154, 2017.

[19] L. de Paula Veronese, C. Badue, F. Auat Cheein, J. Guivant, and A. F. De Souza, "A single sensor system for mapping in gnss-denied environments," *Cognitive Systems Research*, vol. 56, pp. 246–261, 2019.

[20] J. S. McCabe and K. J. DeMars, "Particle filter methods for space object tracking," in *AIAA/AAS Astrodynamics Specialist Conference*, 2014, p. 4308.

[21] R. Linares, J. L. Crassidis, and M. K. Jah, "Particle filtering light curve based attitude estimation for non-resolved space objects," in *AAS/AIAA Space Flight Mechanics Meeting*, 2014, pp. 14–210.

[22] J. Xi, D. Wen, Z. Song, W. Gao, M. Kang, J. Mou, P. Pang, H. Lu *et al.*, "A maximum projection and particle filtering algorithm for space debris detection," *J. Inf. Computational Sci*, vol. 12, pp. 161–169, 2015.

[23] C. Ma, Z. Zheng, J. Chen, and J. Yuan, "Jet transport particle filter for attitude estimation of tumbling space objects," *Aerospace Science and Technology*, vol. 107, p. 106330, 2020.

[24] E. Kraft, "A quaternion-based unscented Kalman filter for orientation tracking," in *Proceedings of FUSION 2003*, vol. 1. IEEE, 2003, pp. 47–54.

[25] J. A. Rebollo, R. Vazquez, F. Gavilan, J. Cordero, and J. Jimenez, "A simmetry-based unscented particle filter for state estimation of a ballistic vehicle," in *IFAC World Congress 2023*, 2023.

[26] B. Wie, *Space Vehicle Dynamics and Control*, 3rd ed. AIAA, 11 2015.

[27] I. N. Bronshtein and K. A. Semendyayev, *Handbook of mathematics*. Springer Science & Business Media, 2013.

[28] R. Rudin, "Strapdown stabilization for imaging seekers," in *Annual Interceptor Technology Conference*, 1993, p. 2660.

[29] K. Tae-Hun, K. Jong-Han, and K. Philsung, "New guidance filter structure for homing missiles with strapdown IIR seeker," *International Journal of Aeronautical and Space Sciences*, vol. 18, no. 4, pp. 757–766, 12 2017.

[30] F. Clarke, "On the inverse function theorem," *Pacific Journal of Mathematics*, vol. 64, no. 1, pp. 97–102, 5 1976.

[31] R. A. Johnson, D. W. Wichern *et al.*, *Applied multivariate statistical analysis*. Prentice hall Upper Saddle River, NJ, 2002.

[32] N. J. Gordon, D. J. Salmond, and A. F. Smith, "Novel approach to nonlinear/non-Gaussian Bayesian state estimation," *IEE proceedings F*, vol. 140, no. 2, pp. 107–113, 1993.

[33] A. Gelb, *Applied Optimal Estimation*. The MIT Press, 5 1974.

[34] F. Gavilan, R. Vazquez, and E. F. Camacho, "An iterative model predictive control algorithm for UAV guidance," *IEEE Transactions on Aerospace and Electronic Systems*, vol. 51, no. 3, pp. 2406–2419, 2015.

[35] S. S. Chin, *Missile Configuration Design*. McGraw-Hill, 1961.

[36] Z. Zhou, Y. Zhong, C. Zeng, and X. Tian, "Attitude estimation using parallel quaternion particle filter based on new quaternion distribution," *Transactions Of The Japan Society For Aeronautical And Space Sciences*, vol. 64, no. 5, pp. 249–257, 2021.

Jose A. Rebollo received a B.Sc. degree in aerospace engineering from the University of Seville and is currently pursuing a double M.Sc. degree in aeronautical engineering and space engineering respectively from University of Seville and Politecnico de Milano and a B.Sc. degree in Physics from the Spanish Open University (UNED).

His research interests include estimation, control, numerical simulation and embedded systems implementation with application to aeronautics and astronautics.

Francisco Gavilan received the M. Eng. and Ph.D. degrees in aerospace engineering from University of Seville, Spain, in 2007 and 2012 respectively. From 2007 to 2012, he was Assistant Professor with the Aerospace Engineering Department, University of Seville, and since 2012 an Associate Professor in the same department. His research interests include applied control to aerospace vehicles, UAV design, and orbital mechanics. He is coauthor of more than 25 journal and conference publications.

Rafael Vazquez (Senior Member, IEEE) received the electrical engineering and mathematics degrees from the University of Seville, Seville, Spain, and the M.Sc. and Ph.D. degrees in aerospace engineering from the University of California, San Diego.

He is currently Professor in the Aerospace Engineering Department and director of the Space Surveillance Chair at the University of Seville, Spain. His research interests include control theory, estimation, distributed parameter systems, and optimization, with applications to spacecraft and aircraft guidance, navigation and control, and space surveillance and awareness. He is coauthor of more than 150 journal and conference publications and the book Control of Turbulent and Magnetohydrodynamic Channel Flows (Basel, Switzerland: Birkhauser, 2007).

Dr. Vazquez currently serves as Associate Editor for Automatica and IEEE Control Systems Letters (L-CSS).